Journal of Mines, Metals and Fuels, *73(9): 2871-2879; 2025. DOI: 10.18311/jmmf/2025/50288*

Print ISSN : 0022-2755

Journal of Mines, Metals and Fuels

Contents available at: *www.informaticsjournals.co.in/index.php/jmmf*

Nanoparticle-Assisted Enhancement of Liquid Crystalline Material Properties: Structural and Optical Characterization

P. Jayaprada[1], K. Sivaram[2], M.C. Rao[3]*, K. Koteswara Rao[4], R. Naveen[5], Sis. Arpuda Jayaseeli[6], V. Naveen Kumar[7], K. Padma Pavani[8] and P. S. Brahamanadam[9]*

[1]Department of Physics, Dhanekula Institute of Engineering and Technology, Vijayawada -521139, Andhra Pradesh, India
[2]Department of Physics, D.M.S.S.V.H. College of Engineering, Machilipatnam - 521001, Andhra Pradesh, India
[3]Department of Physics, Andhra Loyola College, Vijayawada - 520008, Andhra Pradesh, India; raomc72@gmail.com
[4]Department of Physics, Swarnandhra College of Engineering and Technology, Seetharampuram, Narasapur - 534280, Andhra Pradesh, India
[5]Department of Physics, Government Polytechnic for Women, Warangal - 506007, Telangana, India
[6]Medical Surgical Department, Immaculate Institute of Health Sciences, Karaikal - 609607, Puducherry, India
[7]Department of Basic Sciences and Humanities, Seshadri Rao Gudlavalleru Engineering College, Gudlavalleru - 521356, Andhra Pradesh, India
[8]Department of Physics, Vishnu Institute of Technology (A), Bhimavaram - 534202, Andhra Pradesh, India
[9]Physics and R and D Cell, Shri Vishnu Engineering College for Women (A), Bhimavaram - 534202, Andhra Pradesh, India; dranandpotula@svecw.edu.in

Abstract

The strategic incorporation of Zinc Oxide (ZnO) nanoparticles into functional materials such as Liquid Crystalline (LC) systems is crucial for advancing material optimization, refining processes, and resource-efficient recovery. Understanding how nanoparticle dispersion affects structural ordering and optical behavior enables better control over processing dynamics, contributing to sustainable and high-performance material development for industrial applications.

Major Findings: *The study evaluated ZnO-doped nematic LC mixtures (4ba + 4oba) using SEM-EDS, FTIR, POM, and PL techniques across 1-2.5 wt% concentrations. The results demonstrated uniform ZnO dispersion and notable modifications in molecular alignment and emission characteristics. These changes indicate improved structural control and tunable optical behavior, enhancing the potential of such systems in refining, recovery, and precision material processing applications.*

Keywords: *Order Parameter, POM, PL, SEM, ZnO NPs, 4ba+4oba Mixture*

1.0 Introduction

The special class of materials related to soft matter physics in which the molecules exist in both properties, like order and mobility, and show long-range orientation orders, is named as liquid crystals[1,2]. Different properties like optical and scattering of the materials of liquid crystals exhibit different phases, such as nematic and smectic, depending

*Author for correspondence

on the size of the molecules[3]. Different thermodynamic properties of Liquid Crystalline (LC) materials give more information not only about the physical properties but also explain various applications in several branches of science and technology. Liquid crystals are mainly useful in display technology and also in different electro-optical devices, owing to their unique magnetic, electrical, and optical properties[4]. The combined effect of liquid crystals and Nanoparticles (NPs) gives significant attention and a new impact on the liquid crystal research[5,6].

Recent advances have shown that Nanoparticle (NP) doping significantly modifies the physical behavior of LCs, influencing properties like phase transition, molecular orientation, and optoelectronic performance[7,8]. Notably, ZnO Nanoparticles (NPs) have demonstrated their utility in optical devices, including sensors and superconductors[9,10], while their tribological impact and interaction with soft matter systems have been actively studied[11-13].

ZnO NPs play a vital role in the applications of optical devices like gas sensors, chemical sensors, bio-sensors, and superconductors[14,15].

Due to the dispersion of ZnO NPs, the phase transition temperature is reduced at which the phase changes from isotropic to nematic phase in nematic liquid crystals[16]. Also, researchers found that due to the dispersion of ZnO NPs in liquid crystals, absorbance and enthalpy values are varied[17-21]. A range of synthesis methods has been developed for oxide-based nanomaterials, characterized by their flexibility, cost-efficiency, operational simplicity, and ability to yield reproducible quality[22-27]. The mixture of 4ba+4oba LC compound contains only the Nematic (N) phase over a wide temperature range. The studies related to structural, optical, and birefringence were investigated with the impact of ZnO NPs in various concentrations (1-2.5 wt %) in a mixture of 4ba+4oba LC compound.

2.0 Materials and Methods

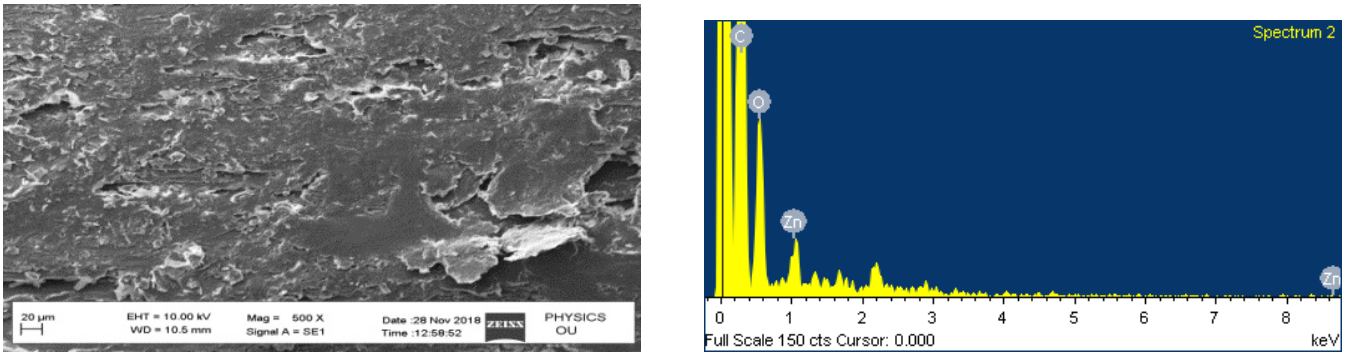
The chemicals such as p-(n-butyl) (4ba) and p-(n-butyloxy) (4oba) benzoic acids used in the present work were taken from the Sigma Aldrich Laboratories, USA. For the preparation of ZnO NPs, high high-pressure combustion method was used. The ingredients of 100 mg of benzoic acid (4ba+4oba) were taken separately. At first, 100 mg of 4ba LC compound was taken in a 5 ml beaker, and ethyl alcohol was mixed with the sample. After that, the sample of 4ba was stirred (700 revolutions/minute) for about 1 h at an ambient temperature of 60 °C with the help of a magnetic stirrer. For the above sample, 100 mg of another liquid crystal named by 4oba compound was added to it. Ethyl alcohol was also added and stirred for about 45 min at an ambient temperature of 60 °C. Later, 1wt% of ZnO NPs were introduced in the mixture of both 4ba and 4oba LC compounds, and further the temperature was raised to nearly 100 °C, then alcohol was evaporated, the homogenous mixture of LC nanocomposite of 4ba+4oba was prepared in the isotropic state. The remaining concentrations of 1.5 to 2.5 wt% ZnO NPs were followed for the above mixture of LC compound[28].

Surface morphological studies were done using SEM (Zeiss special addition -18 make). It has high magnification, large depth, and also strong stereoscopic vision. Through EDS, the chemical elements and confirmation of their relative abundance were examined. The tool Polarizing Optical Microscope (POM-SDTECHS, made SDVPM2727) was used to observe the transition temperatures of the nematic phase of the LC mixture, 4ba+4oba. The FTIR technique was used to measure the various bands inside the prepared sample and analysis of functional group, if present, or bending and stretching of bonds in finger fingerprint region using a Perkin Elmer-spectrum 100 FT-IR spectrometer. Photoluminescence studies were recorded with a 450 W Light Xenon Source on JobinYvonFluorimeter-FL3-11 Spectro-fluorometer. The PL spectra were recorded in the wavelength range from 300 to 750 nm. The PL excitation wavelength monitored was 320 nm. The order parameters of the mixture were determined by the three optical methods, namely Kuczynski, Haller, and effective geometry in the stabilized nematic region at various wavelengths (460, 500, 570, and 635nm), respectively.

3.0 Results and Discussion

3.1 SEM Analysis

SEM is used to determine the size, shape, morphological, and structural information of the sample[29]. Figures 1 (a) and (b) represent the SEM and EDS data of 2.5 wt% dispersed ZnO NPs in the mixture of 4ba+4oba LC compound. EDS gives the information about chemical composition and weight percentages of elements present in the sample, like Zn, O, and C are analyzed[28].



(a) **(b)**

Figure 1. **(a)** SEM image **(b)** EDS data of 2.5 wt% dispersed ZnO NPs in 4ba+4oba LC compound

3.2 POM Studies

The images obtained from the POM confirm whether the crystal is optically isotropic or anisotropic, and also explain whether the crystal is optically positive or negative. The textures are studied with a CCD camera connected to the POM, which reduces the temperature in the isotropic state. The textural images of the LC compound of pure 4ba+4oba, and with 2.5 wt% dispersed ZnO NPs in of 4ba+4oba compounds nematic phase are shown in Figure 2. The POM contains a heating block, which is always maintained with temperature accuracy ± 0.1 °C and magnification 10X. The temperature variation of the heating block is maintained with a voltage variac[28].

3.3 FTIR Studies

This technique is used to identify the different types of materials, like organic, inorganic, or polymeric, and to know the chemical properties of materials whenever the IR radiation is incident on them. The FTIR spectra of pure 4ba+4oba and with 2.5 wt% dispersed ZnO NPs in 4ba+4oba of the LC compound in the wave number range 500-4000 cm^{-1} are shown in Figure 3. The peaks at 2928.79 cm^{-1} and 2852.72 cm^{-1} are related to the OH bond. The peak at 1678.07 cm^{-1} is related to benzoic acid. The peak at 1610.56 cm^{-1} is related to ring stretching, and the peak at 1284.59 cm-1 is related to the dimer. The peak at 1174.65 cm^{-1} is related to CH-OH bending, and the peak at 937.47 cm-1 is ascribed to stretching ring vibration out of plane. The peak at 1693.50 cm^{-1} is related to ZnO stretching.

3.4 Photoluminescence Studies

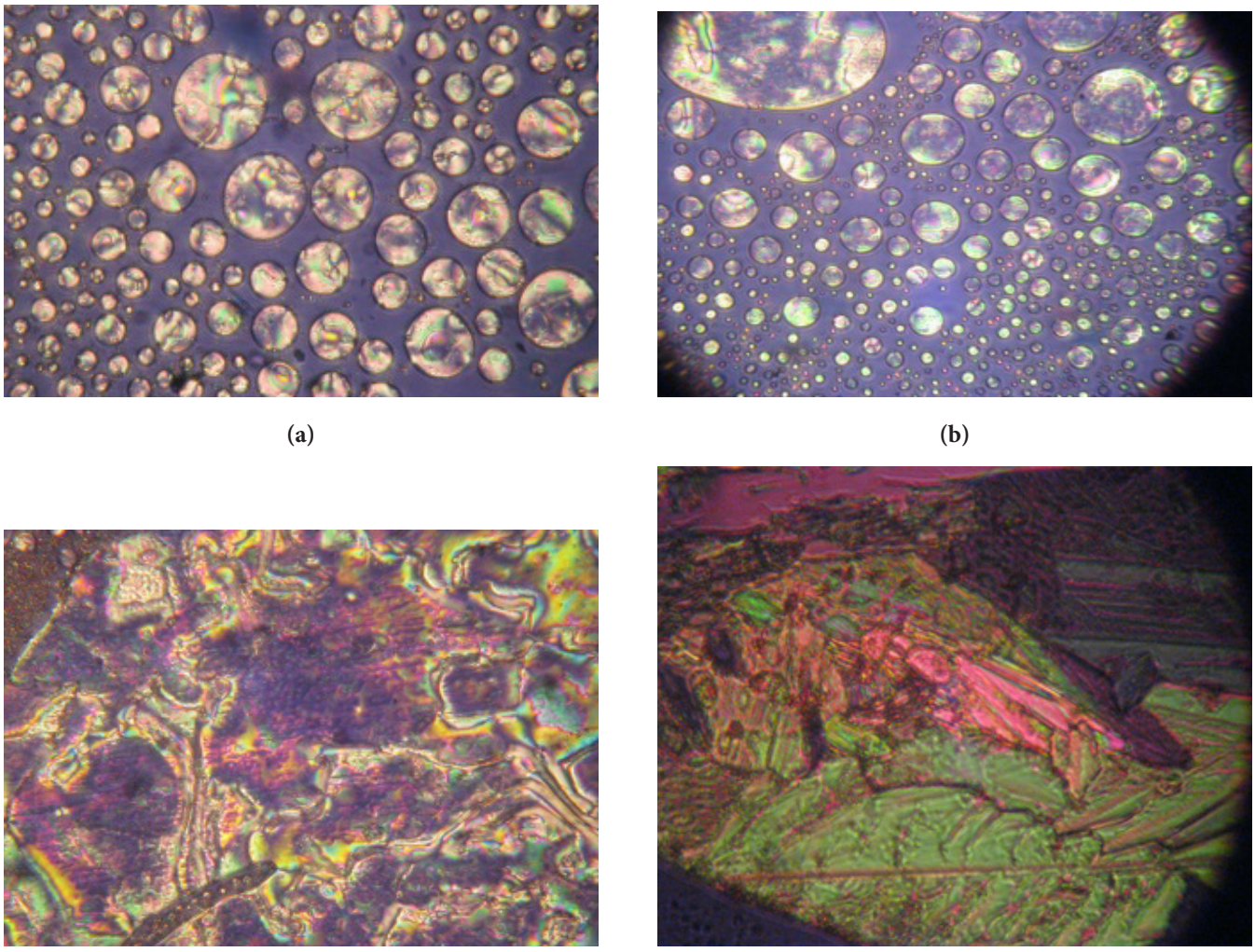
The graph, which is drawn between wavelength and intensity of emitted light, results in a photoluminescence spectrum. Figure 4 shows the photoluminescence spectra of the LC mixture of pure 4ba+4oba and with 2.5wt% dispersed ZnO NPs in 4ba+4oba in the wavelength range 300 -750nm. It contains two peaks; one is at 371 nm, about 4ba+4oba pure, and the other is at 616 nm due to 2.5 wt% dispersed ZnO NPs in 4ba+4oba. The intensity of 2.5 wt% of ZnO dispersed 4ba+4oba LC compound is enhanced due to the dispersion of ZnO NPs compared to the pure mixture. The peak observed at 371 nm is due to the near band edge, i.e., near band emission of free excitons. The shallow donor level of oxygen vacancies could produce the blue emission band at zinc interstitials[30,31]. The other peak observed at 616 nm is due to the presence of point defects within the band gap, like vacancies and interstitials, known as Deep-Level Emission (DLE).

3.5 Evaluation of Order Parameter

The order parameter (S) is nothing but the average direction, which is always oriented about the optic axis in LC molecules. The values of S are measured from the values of Refractive Index (RI) data by various procedures, namely Kuczynski, Vuks, Haller, and also from effective geometry methods. The ZnO NPs play an important role in ordering the LC systems. An improvement in the alignment of the molecules of LCs can be achieved due to the induced ZnO NPs in the 4ba+4oba LC mixture.

3.6 Kuczynski Model

For the measurement of S values, the birefringence (δn) values are taken in the nematic phase and not by the local field experienced by molecules of liquid crystals. The way of finding of S values is so easy, and this model was developed by Kuczynski. The birefringence



(a) **(b)**

(c) **(d)**

Figure 2. **(a)** Isotropic-nematic at 138.2 °C, **(b)** Nematic at130.6° C at 92.7° °C **(c)** Nematic at 125.7 °C, (**d**) Nematic-to-solid textures of 4ba+4oba with dispersion of 2.5 wt% ZnO NPs.

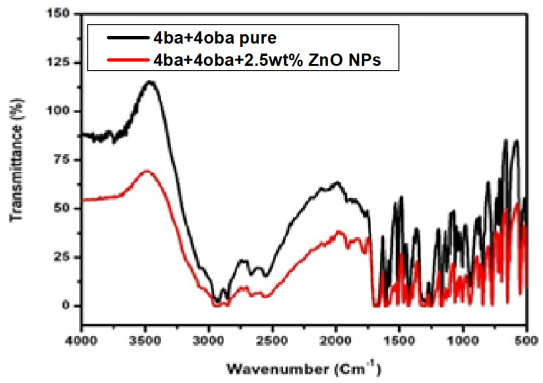


Figure 3. FTIR spectra of 4ba+4oba pure and with dispersion of 2.5 wt% ZnO NPs in 4ba+4oba.

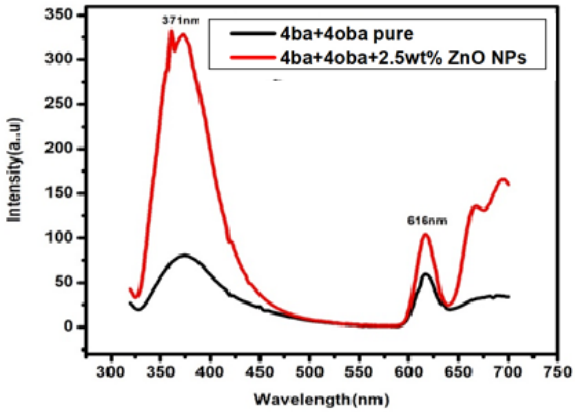


Figure 4. Photoluminescence spectra of 4ba+4oba pure and with dispersion of 2.5 wt% ZnO NPs in 4ba+4oba.

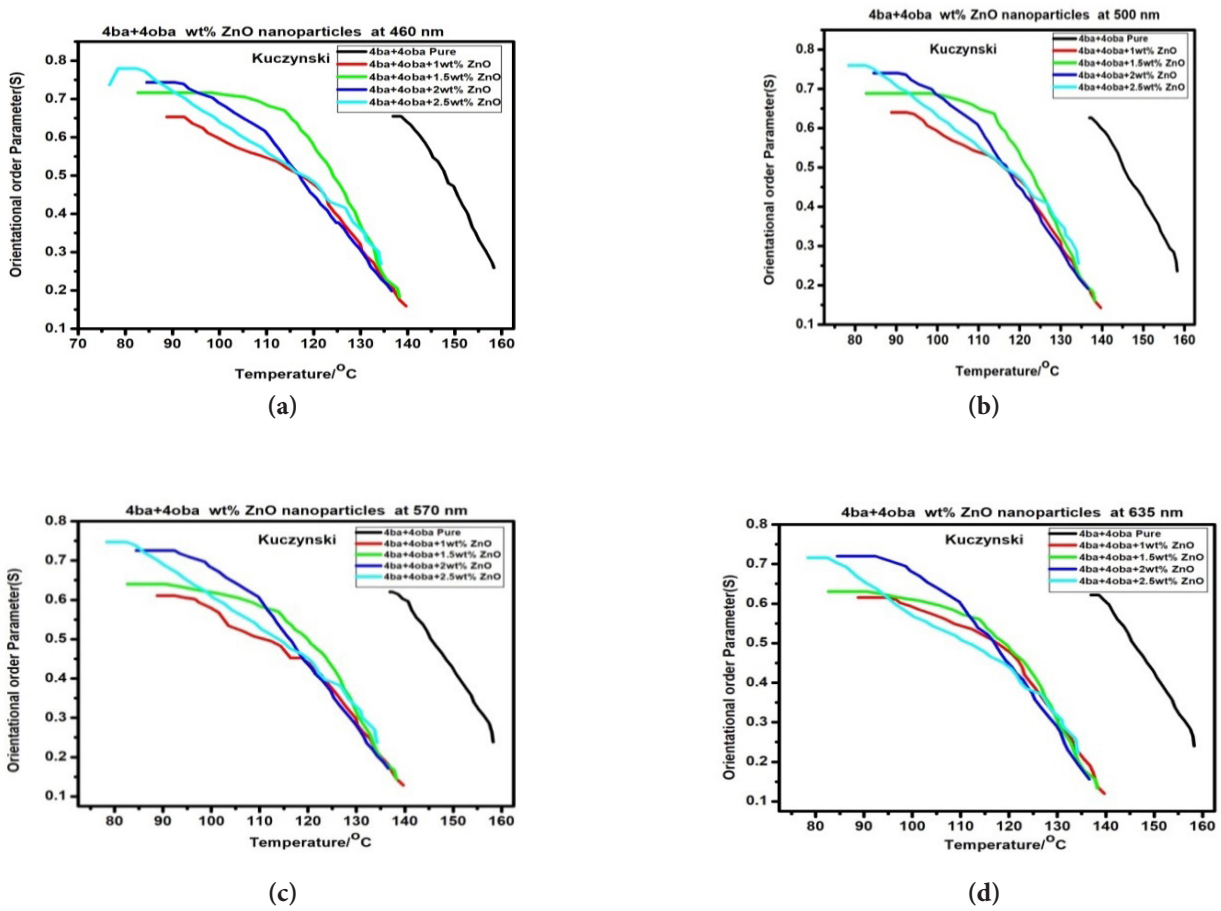


Figure 5. Temperature *vs* order parameter of 4ba+4oba pure with different concentrations at various wavelengths by the Kuczynski model.

is determined by a simple equation, and it is related to temperature; $\delta n = \Delta n.\{1 - (T/T^*)\}^{\beta}$. For fitting these parameters, the value of δn is taken in log form so that it can be written as:

$$\text{Log } \delta n = \log \Delta n + \beta \log \{1 - (T/T^*)\} \quad (1)$$

The simplest equation of measurement of value of order parameter S is $S = \delta n/\Delta n$, in these terms, the special names like Δn are the birefringence in perfect order, $\delta n = (n_e - n_o)$. Here, the values are determined only in the nematic phase. The corresponding order parameters calculated are shown in Figure 5.

3.7 Haller Model

As the birefringence value is increased, the order parameter is also increased, and it is in a linear relationship. The values of S are calculated using Haller's model with a simple equation and it is temperature dependent. The equation is mentioned below. The order parameters calculated by this model are shown in Figure 6.

$$S_{Haller} = \left(1 - \frac{T}{T_{NI}}\right)^{\beta} \quad (2)$$

Where T_{NI} represents the clearing temperature of the Isotropic-Nematic phase, and β is the slope. These values are meant for the perfectly liquid crystalline state of LC materials of order S=1, which thermally influences the behavior of LC materials.

3.8 Effective Geometry Model

α_{eg} is the ratio of n_o/n_e, from the below-mentioned equation, the order parameter can be calculated by this model is named as effective geometry. The corresponding order parameters calculated are shown in Figure 7.

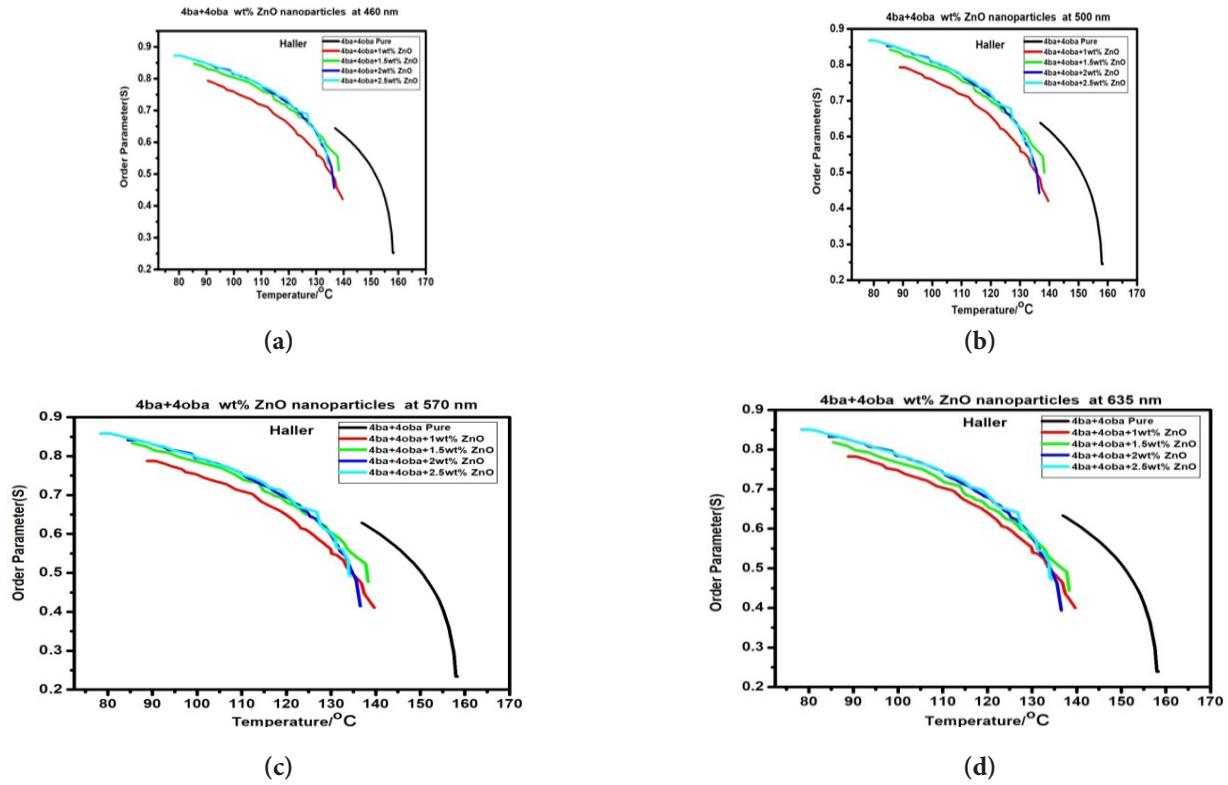


Figure 6. Temperature vs order parameter of 4ba+4oba pure with different concentrations at various wavelengths by Haller model.

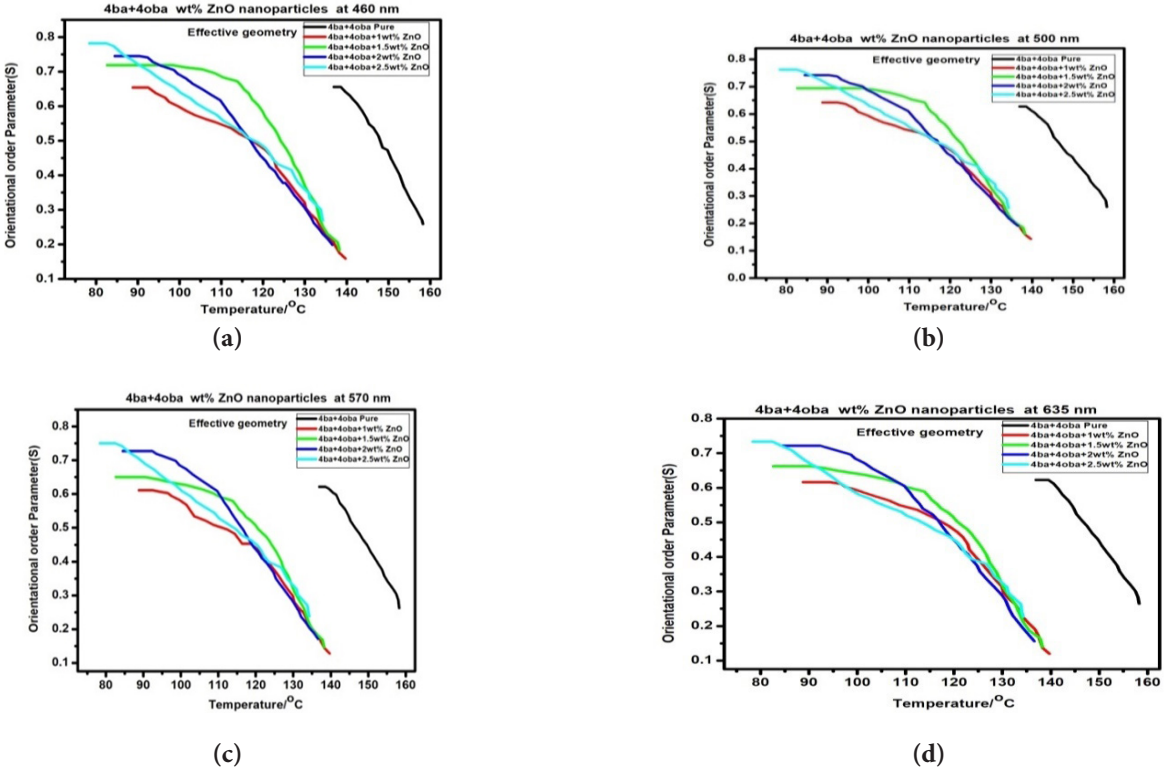


Figure 7. Temperature *vs* order parameter of 4ba+4oba pure with different concentrations at various wavelengths by the effective geometry model.

Table 1. The values of the order parameter of molecules of the LC mixture of 4ba+4oba with dispersed ZnO NPs at various weights by different field models

LC Compound + ZnO NPs	Wavelength in nm	Values of Order Parameter by		
		Kuczynski	Haller	Effective Geometry
4ba+4oba pure	460	0.6250	0.6445	0.6260
	500	0.6066	0.6388	0.6075
	570	0.6004	0.6289	0.6013
	635	0.6002	0.6330	0.6008
4ba+4oba+1 wt%	460	0.6533	0.7936	0.6544
	500	0.6450	0.7931	0.6416
	570	0.6251	0.7878	0.6113
	635	0.6151	0.7824	0.6162
4ba+4oba+1.5 wt%	460	0.7161	0.8478	0.7185
	500	0.6884	0.8430	0.6941
	570	0.6397	0.8332	0.6621
	635	0.6305	0.8184	0.6501
4ba+4oba+2 wt%	460	0.7433	0.8577	0.7452
	500	0.7399	0.8523	0.7416
	570	0.7256	0.8414	0.7272
	635	0.7197	0.8323	0.7213
4ba+4oba+2.5 wt%	460	0.7797	0.8729	0.7819
	500	0.7603	0.8681	0.7622
	570	0.7468	0.8583	0.7504
	635	0.7163	0.8506	0.7213

$$S_{\alpha eg} = \frac{3\sqrt{\langle n^2 \rangle}}{(\Delta n)_o}\left(\frac{1-\alpha_{eg}}{1+2\alpha_{eg}}\right) \quad (3)$$

The order parameters of 4oba+4ba LC compound are increased with different wt% concentration of ZnO NPs. Further, the order parameter values are also improved from higher wavelengths to lower wavelengths in the visible region in the three internal field models[28]. From the above observations, since the ZnO NPs are larger and high dipole moment, they can produce more torque than nematic liquid crystals[32,33]. This torque is used to orient the molecules of liquid crystals, which enhances the birefringence and ordering of liquid crystal molecules. The ordering of the LC system is calculated with the three internal field models and also observed with induced ZnO NPs (1-2.5 wt%). Various research studies have found that parameters like electrical conductivity, birefringence, and photoluminescence are increased with the dispersion of ZnO NPs in LC material[34-36]. The optical parameters play a significant role in display technology. The related data is presented in Table 1.

4.0 Conclusion

The samples of LC mixtures of p-(n-butyl) and p-(n-butyloxy) benzoic acids with the homogeneous dispersion of ZnO NPs in different wt% (1-2.5 wt%) were prepared. Different characterization techniques like SEM, POM, FTIR, PL, and calculation of order parameters were undertaken for 4ba+4oba pure and 2.5 wt% ZnO dispersed LC mixtures. The morphological studies and elemental analysis were done by SEM and EDS data. SEM image showed nanoparticle dispersion with LC material presented and the EDS data gave chemical analysis of different elements involved in the sample. The images of different textures of nematic phase of pure and nanodispersed LC compounds were examined by POM. From POM, the transition temperatures of pure LC materials with dispersion of ZnO NPs were measured and compared with the DSC results. From FTIR, the vibrational and rotational frequencies were observed corresponding to the different bonds formed by the LC molecules with dispersion of NPs in the sample. The photoluminescence studies showed the enhancement in the intensity of pure 4ba+4oba than 2.5 wt% ZnO NPs in

4ba+4oba LC mixture. The optical anisotropy and the order parameter values were enhanced with the dispersion of NPs and also achieved wide angle vision. The increase of order parameter and other optical properties like luminescence of the samples prepared revealed that they may be useful in building blocks of LC display devices.

5.0 Acknowledgement

The authors sincerely thank their College Managements for their valuable infrastructural facilities that enabled us to complete this research.

6.0 Author Contributions

All authors have contributed significantly to this research. Dr. M. C. Rao and Dr. P. S. Brahmanandam conceptualization and supervised the research. All authors reviewed and approved the final manuscript.

7.0 References

1. Collings PJ, Hird M. Introduction to liquid crystals chemistry and physics. Taylor and Francis. 1997.
2. Singh S. Liquid crystal fundamentals. World Scientific; 2002.
3. Dmitriev SM, Dick VP, Kostyuk NN, *et al*. Experimental studies of light-wave phase shift by polymer dispersed liquid crystal films. SPQEO. 2010; 13(2):132-136. https://doi.org/10.15407/spqeo13.02.132
4. Chandrasekhar S. Liquid crystals. 2nd Edition. Cambridge University Press; 1992.
5. Hegmann T, Qi H, Marx VM. Nanoparticles in liquid crystals: Synthesis, self-assembly, defect formation and potential applications. J Inorg Organomet Polym Mater. 2007; 17(3):483-508. https://doi.org/10.1007/s10904-007-9140-5
6. Bisoyi HK, Kumar S. Liquid-crystal nanoscience: an emerging avenue of soft self-assembly. Chem Soc Rev. 2011; 40(1):306-319. https://doi.org/10.1039/B901793N
7. Alamiery AA. Synthesized heterocyclic compounds as corrosion inhibitors for steel in acidic environments: A mini-review. JME. 2024; 2(4):235-249. https://doi.org/10.61552/JME.2024.04.001
8. Prozhega M, Reschikov E, Konstantinov E. The technological factors and operating conditions influence on the molybdenum disulfide coatings tribological properties. JME. 2023; 1(4):159-163. https://doi.org/10.61552/JME.2023.04.003
9. Bello SA, Kolawole MY, Balogun SW, Agunsoye JO, Hassan SB. Effects of applied loads and aluminium nanoparticle additions on wear resistance properties of particle reinforced epoxy nanocomposites. JME. 2023; 1(4):137-146. https://doi.org/10.61552/JME.2023.04.001
10. Abbass MK, *et al*. Friction stir processed Al-SiC-Al_2O_3 hybrid surface Composites functional nanoparticle-based composite surfaces; 2023
11. Ishii R, Miwa R, Miyanaga N, Tomioka J. Effect of cross-sectional profile of circular dimples on hydrodynamic lubrication characteristics of thrust bearings. JME. 2023; 1(1), 21-25. https://doi.org/10.61552/JME.2023.01.003
12. Fedorov SV. The mystery and clarity of Leonardo da Vinci's coefficient of friction. JME. 2023; 1(1):8-20. https://doi.org/10.61552/JME.2023.01.002
13. Prusov E, Aborkin A, Deev V, Bokaryov D, Babin D. Tribological behavior of cast aluminum matrix composites after multiple remelting. JME. 2023; 1(3):131-135. https://doi.org/10.61552/JME.2023.03.006
14. Gupta SK, Joshi A, Kaur M. Development of gas sensors using ZnO nanostructures . J Chem Sci. 2010; 122:57-62. https://doi.org/10.1007/s12039-010-0006-y
15. Zhao Z, Lei W, Zhang X, Wang B, Jian H. ZnO-Based Amperometric Enzyme Biosensors. Sensors. 2010; 10:1216-1231. https://doi.org/10.3390/s100201216
16. Banu SR, Subhan CM, Dinesh R, Fakruddin K. Influence of TiO_2 and ZnO nanoparticles on orientational order parameter of LC compounds - An optical study. Mol Cryst Liq Cryst. 2018; 665(1):238-247. https://doi.org/10.1080/15421406.2018.1495867
17. Sharma A, Malik P, Dhar R, Kumar P. Improvement in electro-optical and dielectric characteristics of ZnO nanoparticles dispersed in a nematic liquid crystal mixture. Bull Mater Sci. 2019; 42(215). https://doi.org/10.1007/s12034-019-1902-5
18. Brouckaert N, Podoliak N, Orlova T, Bankova D, Fazio AFD, *et al*. Nanoparticle-Induced Property Changes in Nematic Liquid Crystals. Nanomaterials. 2022; 12(3):341. https://doi.org/10.3390/nano12030341
19. Onsal G, Kaynar UH. Synthesis of doped ZnO nanoparticles and their effect on the dielectric and electro-optical characterization of nematic liquid crystals. J Electron Mater. 2023; 52:2569-2579. https://doi.org/10.1007/s11664-023-10219-x
20. Kaur G, Khushboo, Malik P. Mesomorphic, electro-optic and dielectric behavior of self-assembled nanocomposite materials: Nematic mixture doped with carbon coated

cobalt nanoparticles. J Mol Liq. 2022; 351:118639. https://doi.org/10.1016/j.molliq.2022.118639
21. Kanwar A, Ghodke S, Gajghate V. Determination of Refractive Index and Birefringence of Nanoparticle-Doped Liquid Crystals. Int J Thermophys. 2023; 44(35). https://doi.org/10.1007/s10765-022-03145-3
22. Ravindranadh K, Babu B, Rao MC, *et al*. Structural and photoluminescence studies of Co^{2+} doped Ca-Li hydroxyapatite nanopowders. J Mater Sci Mater Electron. 2015; 26(9):6667-6675. https://doi.org/10.1007/s10854-015-3268-9
23. Rao M. C, Ravindranadh K, Shekhawat MS. Synthesis and applications of CdSe nanoparticles. AIP Conf Proc. 2013; 1536(1):215-216. https://doi.org/10.1063/1.4810177
24. Rao MC, Begum SKM, Reddy ES, Hussain OM. Electrical conduction behavior of $LiNi_xCo_{1-x}O_2$ thin films. AIP Conf Proc. 2012; 1447:613-614. https://doi.org/10.1063/1.4710152
25. Ravindranadh K, Babu B, Reddy CV, Shim J, Rao MC, *et al*. EPR andoptical studies of Fe^{3+} -doped Ca-Li hydroxyapatite nanopowder: Mechanochemical synthesis. Appl Magn Reson. 2015; 46:1-15. https://doi.org/10.1007/s00723-014-0613-8
26. Rao MC. Microstructural and electrochemical properties of $LiNi_xCo_{1-x}O_2$ thin films prepared by pulsed laser deposition. J Optoelectron Adv Mater. 2010; 12(12):2433-2436.
27. Sreeram N, Aruna V, Koutavarapu R, Lee DY, Rao MC, Shim J. Fabrication of $InVO_4$ /$SnWO_4$ heterostructured photocatalyst for efficient photocatalytic degradation of tetracycline under visible light. Environ Res. 2023; 220:115191. https://doi.org/10.1016/j.envres.2022.115191
28. Jayaprada P, Pardhasaradhi P, Madhav BTP, Reddy KK, *et al*. Studies on birefringence, order parameter and image analysis of liquid crystalline p-n butyloxy/butyl benzoic acid with dispersed ZnO nanoparticles. Z Naturforsch A. 2021; 76(1):75-98. https://doi.org/10.1515/zna-2020-0198
29. Newbury DE, Joy DC, Echlin P, Fioriand CE, Goldstein JI. Advanced scanning electron microscopy and X-ray microanalysis. Plenum Press; 1986.
30. Oba F, Nishitani SR, Isotani S, Adachi H, Tanaka I. Energetics of native defects in ZnO. J Appl Phys. 2001; 90 (2):824-828. https://doi.org/10.1063/1.1380994
31. Kumar V, Singh N, Kapoor A, Ntwaeaborwa OM, *et al*. Effect of annealing on the structural, morphological and photoluminescence properties of ZnO thin films prepared by spin coating. J Colloid Interface Sci. 2014; 428:8-15. https://doi.org/10.1016/j.jcis.2014.04.035
32. Jung HY, Kim HJ, Yang S, Kang YG, *et al*. Enhanced electro-optical properties of Y_2O_3 (yttrium trioxide) nanoparticle-doped twisted nematic liquid crystal devices. Liq Cryst. 2012; 39(7): 789-793. https://doi.org/10.1080/02678292.2012.681073
33. Kim HJ, Kang YG, Park HG, Lee KM, *et al*. Effects of the dispersion of zirconium dioxide nanoparticles on high performance electro-optic properties in liquid crystal devices. Liq Cryst. 2011; 38(7):871-875. https://doi.org/10.1080/02678292.2011.584637
34. Sonali MK, Pisharody GR, Kulkarni SD, Bhagavath P. H-bonded liquid crystals: Effect of ZnO nanoparticles on the enhancement in electrical conductivity. Nano Ex. 2025; 6:015013. https://doi.org/10.1088/2632-959X/adb5a6
35. Sonali MK, Kulkarni SD, Lewis PM, *et al*. Mixed ionic-electronic conductivity in ZnO doped tunable soft materials. Discov Appl Sci. 2025; 7(138). https://doi.org/10.1007/s42452-025-06559-4
36. Chen CH, Dierking I. Nanoparticles in thermotropic and lyotropic liquid crystals. Front Soft Matter. 2025; 4:1518796. https://doi.org/10.3389/frsfm.2024.1518796